Cell wall remodeling at the fission yeast cell division site requires the Rho-GEF Rgf3p

Jennifer L. Morrell-Falvey*,‡, Liping Ren*, Anna Feoktistova, Greg Den Haese and Kathleen L. Gould§

Howard Hughes Medical Institute and Department of Cell and Developmental Biology, Vanderbilt University Medical Center, Nashville, TN 37232, USA

*These authors contributed equally to this work
‡Present address: The Oak Ridge National Laboratory, Life Sciences Division, Oak Ridge, TN 37831, USA
§Author for correspondence (e-mail: kathy.gould@vanderbilt.edu)

Accepted 24 August 2005
Journal of Cell Science 118, 5563-5573 Published by The Company of Biologists 2005
doi:10.1242/jcs.02664

Summary

Cytokinesis in *Schizosaccharomyces pombe* is accompanied by several stages of cell wall remodeling at the division site. Coincident with actomyosin ring constriction, primary and secondary septa are deposited and then the primary septum is degraded to release daughter cells from one another. These steps require the activities of glucan synthases and glucanases, respectively, which must be coordinated with one another to prevent cell lysis. The *lad1-1* mutation undergoes cell lysis specifically at cell division owing to the absence of the Rgf3p Rho1-guanine nucleotide exchange factor (GEF) at the division site. Electron microscopic analysis indicates that lysis occurs only as the primary septum begins to be degraded. Overproduction of either Rho1p or the previously uncharacterized Rab-GTPase-activating protein (GAP) involved in secretion, Gyp10p, suppresses *lad1-1* lethality. Rgf3p is periodically produced in an Ace2p-dependent manner and localizes to the medial region of the cell early in mitosis, a pattern of expression distinct from the highly related Rho-GEF, Rgf1p. Although *rgf1*$^{+}$ is not an essential gene, it is synthetically lethal with *rgf2*-deleted cells whereas no negative genetic interactions were detected between *rgf2*-deleted cells and *lad1-1*. Our data suggest that the three closely related fission yeast Rho-GEF molecules perform two distinct essential functions. Rgf3p appears necessary to stimulate Rho1p-mediated activation of a glucan synthase crucial after septation for proper new cell-end formation.

Key words: Fission yeast, Cytokinesis, Rho-GEF, Rho1

Introduction

Cytokinesis is the final step of the cell cycle that results in the formation of two daughter cells from one. This process is regulated temporally and spatially such that the replicated and segregated chromosomes are evenly divided between daughter cells. The genetically tractable yeast *Schizosaccharomyces pombe* is an excellent organism for studying cytokinesis as it divides by medial fission following assembly and contraction of an actomyosin-based cleavage apparatus that directs placement and assembly of new membrane and cell wall materials (Balasubramanian et al., 2004; Krapp et al., 2004; Wolfe and Gould, 2005). Furthermore, numerous mutations are available that are defective in each step of the cell division process.

The initial phase of cytokinesis involves establishing the division site at the center of a symmetrical cell. This process begins at the onset of mitosis when components of the actomyosin ring are recruited to the cell cortex immediately overlaying the nucleus (reviewed by Balasubramanian et al., 2004; Wolfe and Gould, 2005). The next steps of cytokinesis, actomyosin ring constriction and septation, require a conserved signaling cascade referred to as the septation initiation network (SIN) that is organized at the spindle pole body, a microtubule-organizing center analogous to the mammalian centrosome (reviewed by Krapp et al., 2004; McCollum and Gould, 2001).

Septation occurs concomitantly with actomyosin ring constriction as the primary septum is laid down in a centripetal manner behind the constricting CAR (reviewed by Le Goff et al., 1999a). Indeed, actomyosin ring constriction does not proceed in the absence of primary septum formation (Le Goff et al., 1999b; Liu et al., 1999). The primary septum consists primarily of unbranched 1,3-β-glucan and 1,3-α-glucan (Humbel et al., 2001) and Cps1p is a 1,3-β-glucan synthase essential for its assembly (Le Goff et al., 1999b; Liu et al., 1999). Secondary septa consisting primarily of branched 1,3-β-glucan, α-galactomannan, and 1,3-α-glucan (Humbel et al., 2001) are deposited flanking the division septum. Final separation of the daughter cells occurs through digestion of the primary septum, carried out at least in part by the endo-β-1,3-glucanase, Eng1p, and the endo-α-1,3 glucanase, Agn1p (Alonso-Nunez et al., 2005; Dekker et al., 2004; Martin-Cuadrado et al., 2003). These gene products are periodically expressed under control of the Ace2p transcription factor at the time of septation (Alonso-Nunez et al., 2005; Peng et al., 2005; Rustici et al., 2004). Efficient septum degradation and cell separation also require the exocyst complex, a MAPK (Pmk1p), a MAPK phosphatase (Pmp1p), calcineurin (Ppb1p), subunits of the mediator complex (Sep10p, Sep11p, and Sep15p), as well as septins and their regulator Mid2p (An et al., 2004; Hall and Russell, 2004; Sipiczki et al., 1993; Sugiura et al., 1998; Tasto et al., 2003; Toda et al., 1996; Wang et al., 2002; Yoshida et al., 1994). Precisely how these proteins are

coordinated to regulate cell wall synthesis and degradation during the division process is not well understood.

Here we present the isolation and characterization of a mutation affecting cell wall remodeling during the final stages of fission yeast cell division termed *lad1-1*. As primary septum degradation begins, *lad1-1* mutant cells expose unprotected membranes adjacent to the septum and consequently, they lyse. We present evidence that this phenotype results from loss of Rgf3p, an essential Rho-GEF molecule, from the division site. The *lad1-1* mutation can be suppressed by overproduction of Rho1p or a Rab GAP molecule. Rgf3p is periodically produced in a manner partially dependent upon the Ace2 transcription factor and joins the actomyosin contractile ring in metaphase. The kinetics of Rgf3p localization raise the possibility that it participates early in the cytokinetic process. A closely related and genetically linked Rho-GEF gene, *rgf1*$^+$, is not essential for the division process and Rgf1p has a distinct pattern of expression and localization. However, Rgf1p becomes essential in the absence of a third related Rho-GEF, Rgf2p. Our data indicate that these three related Rho-GEF molecules perform two distinct essential functions during the cell cycle.

Materials and Methods

Yeast strains, methods and media

Yeast strains used in this study are listed in Table 1. *S. pombe* strains were grown in yeast extract (YE) medium or minimal medium with appropriate supplements (Moreno et al., 1991). Mutagenesis of cells with nitrosoguanidine was performed as described (Moreno et al., 1991). Crosses were performed on glutamate medium (minimal medium lacking ammonium chloride with 0.01 M glutamate, pH 5.6). Random spore analysis and tetrad analysis were performed as described (Moreno et al., 1991). Transformations were performed by electroporation (Prentice, 1992). For regulated expression of genes by the *nmt1* promoter (Maundrell, 1993), cells were grown either in minimal media lacking thiamine to allow expression or with the addition of 5 μM thiamine to repress expression. Double-mutant strains were constructed and identified by tetrad analysis or random spore analysis. In order to test for dominance, the *lad1-1* strain was crossed to a *mei1-102* strain (*mei1-102* mutants will mate with h$^-$ partners, but the resulting diploids will not sporulate) and stable diploids were obtained using complementation of nutritional markers.

To obtain large cultures of synchronized *lad1-1* cells, 4 l of cells were grown to mid-log phase at permissive temperature (25°C) in YE medium. Cells were separated on the basis of size by centrifugal elutriation in an elutriator rotor and the smallest cells, in early G2, were collected and inoculated into YE medium at 25°C or 36°C. Synchrony was monitored at 20-minute intervals by scoring 100 cells for the presence of a septum. For smaller cultures, cells were synchronized by lactose gradient centrifugation as described previously (Barbet and Carr, 1993).

Gene cloning and deletion

A *S. pombe* genomic library constructed in the pUR19 plasmid (Barbet et al., 1992) was introduced into the *lad1-1* strain and transformants were selected on minimal medium, replica plated once to the same medium and then to 36°C on YE medium. Plasmids were isolated from these colonies and the sequences of their inserts determined. Standard cloning procedures were used to make truncations of the gene fragments. These fragments were tested for re-rescue so that the rescuing activity was assigned to the correct open reading frame. For integration mapping, the inserts were cloned into the ura4-based integrating vector pJK210 (Keeney and Boeke, 1994). The resulting plasmids were linearized and transformed into *lad1-1* cells. Stable transformants were selected on media lacking uracil and outcrossed to wild-type and *lad1-1* strains to determine linkage of the rescuing genes with the *lad1*$^+$ locus.

Table 1. *Schizosaccharomyces pombe* strains used in this study

Strain		Genotype	Source
KGY28	h$^-$	972 wild type	Lab. stock
KGY69	h$^+$	975 wild type	Lab. stock
KGY246	h$^-$	*leu1-32 ura4-D18 ade6-M210*	Lab. stock
KGY247	h$^+$	*leu1-32 ura4-D18 ade6-M210*	Lab. stock
KGY249	h$^+$	*leu1-32 ura4-D18 ade6-M216*	Lab. stock
KGY281		*mei1-102 lys1-131*	Lab. stock
KGY1116	h$^-$	*rgf1-GFP::kan^R lad1-1 leu1-32 ura4-D18 ade6-M210*	This study
KGY1117	h$^-$	*rgf3-GFP(lad1-1)::kan^R leu1-32 ura4-D18 ade6-M210*	This study
KGY2030	h$^-$	*lad1-1 leu1-32 ura4-D18 ade6-M210*	This study
KGY2031	h$^+$	*lad1-1 leu1-32 ura4-D18 ade6-M210*	This study
KGY2041	h$^-$	*lad1-1 cdc25-22 leu1-32 ura4-D18 ade6-M210*	This study
KGY2111	h$^+$	*gyp10::ura4$^+$ ura4-D18 leu1-32 ade6-M210 his3-D1*	This study
KGY2547	h$^-$	*lad1-1 swi5-39*	This study
KGY2548	h$^+$	*lad1-1 swi5-39*	This study
KGY2925	h$^+$	*swi5-39 ade6-M210 leu1-32 ura4-D18*	This study
KGY3944	h$^-$	*lad1-1 spn3::ura4 leu1-32 ura4-D18 ade6-M210*	This study
KGY3945	h$^+$	*gyp10::ura4$^+$ ura4-D18 leu1-32 ade6-M210 exo70::ura4$^+$ his3-D1*	This study
KGY4401	h$^-$	*rgf3-myc$_{13}$ leu1-32 ura4-D18 ade6-M210*	This study
KGY4404	h$^-$	*rgf1-GFP::kan^R leu1-32 ura4-D18 ade6-M210*	This study
KGY4407	h$^-$	*rgf3-GFP::kan^R leu1-32 ura4-D18 ade6-M210*	This study
KGY5160	h$^-$	*rgf3-myc$_{13}$ ace2::kan^R leu1-32 ura4-D18 ade6-M210*	This study
KGY5385	h$^+$	*rgf1::ura4$^+$ ura4-D18 leu1-32 ade6-M21X*	This study
KGY5400	h$^-$	*rgf3-GFP::kan^R nda3-km311leu1-32 ura4-D18*	This study
KGY5326	h$^-$	*rgf3-GFP::kan^R sid2-250 leu1-32 ura4-D18 ade6-M21X*	This study
PN1251	h$^+$	*lys1 ade4-31 swi5-39*	Lab. stock
PN1253	h$^-$	*ura1-171 his6-365 swi5-39*	Lab. stock
MBY919	h$^-$	*exo70::ura$^+$ ura4-D18 leu1-32*	M. Balasubramanian*
KMGA1	h$^-$	*rgf2::ura4$^+$ ura4-D18 leu1-32*	M. Miyamoto‡

*Wang et al., 2003; ‡Iwaki et al., 2003.

The *gyp10*$^+$ gene was deleted by using a PCR-generated DNA fragment containing the *ura4*$^+$ gene flanked by 80 bp both upstream and downstream of the ORF (Bahler et al., 1998). The *rgf1*$^+$ and *rgf3*$^+$ genes were deleted using longer flanking regions of homology surrounding the open reading frame that were generated by PCR and cloned on either end of the *ura4*$^+$ gene. The PCR or longer linear DNA fragments containing *ura4*$^+$ were transformed into a diploid *S. pombe* strain and stable Ura$^+$ transformants were selected. These were induced to sporulate by growth on glutamate medium and tetrads were dissected. All four spores from each tetrad of the *rgf1* and *gyp10* heterozygous diploids grew and the two Ura$^+$ colonies were screened by PCR and Southern blotting for the correct gene replacement. To produce GFP-Gyp10p, an *Nde*I site was introduced at the start codon of the *gyp10*$^+$ genomic clone by site-directed mutagenesis using the Bio-Rad Mutagene kit according to manufacturer's instructions. The *gyp10*$^+$ open reading frame and 3′ flanking region were then excised from the genomic clone by digestion with *Nde*I and *Bam*HI and ligated into the pREP series of vectors including pREP81GFP.

The *rgf1*$^+$ and *rgf3*$^+$ genes were tagged at their chromosomal loci at the 3′ ends of their open reading frames with sequences encoding green fluorescent protein (GFP), or 13 copies of the Myc epitope recognized by the 9E10 monoclonal antibody by a PCR-mediated strategy as described previously (Bahler et al., 1998).

Fluorescence microscopy

Fluorescence microscopy was performed using a Carl Zeiss Axioscope and the appropriate set of filters or using Carl Zeiss MicroImaging Axiovert II inverted microscope equipped with an UltraView LCI real-time scanning head confocal (PerkinElmer) and a 488 nm argon ion laser (for GFP excitation). Images were captured on an Orca-ER charge-coupled device camera (Hamamatsu) using Ultra-View software (PerkinElmer) and were then processed using Volocity 2.0 software (Improvision). Calcofluor was used to detect cell wall material in live cells as described (Balasubramanian et al., 1997). Antibodies to Arp3 (McCollum et al., 1996) and actin (Amersham) were diluted 1:100, and detected with Texas-Red-tagged anti-rabbit-IgG and Texas-Red-tagged anti-mouse-IgG antibodies (Molecular Probes) in methanol-fixed cells. DNA was visualized using DAPI as described (Balasubramanian et al., 1997). Strains expressing GFP-tagged proteins were grown in liquid YE medium and visualized live or after ethanol fixation. Septa were visualized by staining ethanol-fixed cells with a 1 mg/ml aniline blue solution (Sigma-Aldrich).

Immunoprecipitation and immunoblotting

Native or denatured cell lysates were prepared in NP-40 buffer as previously described (Gould et al., 1991). Immunoprecipitations were performed with anti-Myc (9E10) antibodies or anti-GFP monoclonal antibody (Roche). Proteins were resolved by electrophoresis on 4-12% NuPAGE gels (Novex), 10% Bis-Tris gels or by 10% SDS-PAGE. Proteins were transferred onto PVDF membranes (Immobilon P; Millipore) for immunoblot analysis performed as previously described (Tasto et al., 2003) with monoclonal anti-PSTAIRE (Sigma-Aldrich), anti-GFP monoclonal (Roche) or the 9E10 monoclonal antibody. Immunoblots were visualized using the Li-Cor Odyssey Infrared Imaging System (Lincoln, Nebraska) according to the manufacturer's suggestions.

Electron microscopy

For EM, 10^6 *lad1-1* cells were fixed 4 hour after shifting to 36°C in 1.5% potassium permanganate. They were then treated with 2% glutaraldehyde and osmium tetroxide, block-stained with uranyl acetate and dehydrated in ethanol series. Cells were embedded in spurr in BEEM capsules, which were polymerized under vacuum at 65°C. Sections were cut to 75 μm with a Leica Ultracut, picked onto grids, stained with uranyl acetate and lead citrate and imaged on a Philips 300 electron microscope at 60 kV.

Results

Isolation of the *lad1-1* mutation that causes lysis specifically at division

The *lad1-1* strain was isolated in a genetic screen for mutants that were unable to form colonies on solid media containing 50 mM NaF, a concentration of NaF permissive for wild-type cell growth (G.D.H. and K.L.G., unpublished). After extensive backcrossing, the *lad1-1* mutant remained sensitive to 50 mM NaF (data not shown) and was also found to be temperature sensitive for growth (Fig. 1A). Following incubation at 36°C on YE medium, *lad1-1* cells arrested growth with a homogeneous phenotype (Fig. 1A). All cells lysed while undergoing division and the daughter cells remained attached to one another. The doublets of lysed cells resembled the shape of boomerangs and the mutant was given the name *lad1-1* for lethal at division. Growth of the *lad1-1* strain at 36°C was rescued by including osmotic stabilizers such as 1.2 M sorbitol or 1.2 M KCl in the YE medium (data not shown). The *lad1-1* strain was also able to form colonies at 36°C on minimal medium agar plates (data not shown).

To determine precisely when *lad1-1* cells lysed, a synchronized population of cells was isolated by centrifugal elutriation at 25°C. One portion of the culture was then shifted to 36°C while another was incubated at 25°C. The septation index was measured every 20 minutes through the first round of septation (Fig. 1B) and cells incubated at 36°C were stained with calcofluor to visualize the cell wall and septum (Fig. 1C). The *lad1-1* cells incubated at 36°C were normal in morphology and underwent septation at the appropriate time (Fig. 1C, panels a-e). However, at the end of cell division but before complete separation of the daughter cells, the cellular contents spilled from the newly created ends of each cell (Fig. 1C, panel f). More than 95% of the cells lysed at this stage of the cell cycle (Fig. 1B).

Because defects in the actin cytoskeleton can confer cell wall defects, the organization of the *lad1-1* actin cytoskeleton was also examined from the synchronized culture. The actin cytoskeleton of *lad1-1* cells was completely normal up to the point of cell lysis (Fig. 1D, panels a and b). Actin patches were concentrated at cell ends prior to mitosis. Actin contractile rings formed normally as *lad1-1* cells entered mitosis, and actin patches localized normally adjacent to the septum (Fig. 1D, panel a). Even following lysis, F-actin patches, detected by staining with antibodies to Arp3p, an actin patch component (McCollum et al., 1996), remained at the newly formed cell ends (Fig. 1D, panel c). These results suggested that the lysis phenotype of *lad1-1* cells was not due to defects in the actin cytoskeleton but was probably due to defects in cell wall formation or remodeling that occurs as cells separate.

To examine whether cell wall defects were specific to dividing *lad1-1* cells, a double mutant of *lad1-1* with *cdc25-22* was constructed and examined after shift to 36°C. Because *cdc25*-22 *lad1-1* cells maintained a typical rod shape and became highly elongated when incubated at 36°C (Fig. 1E), it is unlikely that *lad1*$^+$ function is required for general cell wall synthesis or integrity. We next asked whether inhibiting cell

separation would suppress the cell lysis phenotype of *lad1-1* cells. To examine this, *lad1-1* was combined with the *spn3* deletion allele. In these cells, cell separation is greatly delayed owing to defective septin rings, and *spn3Δ* cells grow as chains of typically two to four cell compartments (An et al., 2004; Berlin et al., 2003; Tasto et al., 2003). In *lad1-1 spn3Δ* cells, cell lysis was indeed suppressed until the chains began to cleave (Fig. 1F). However, the lysis delay did not ultimately rescue growth of the *lad1-1* strain (data not shown).

To more precisely define the defect in *lad1-1* cell walls during cell division, wild-type and *lad1-1* cells that had been shifted to 36°C were examined by electron microscopy. Representative images of our results are presented in Fig. 2. In *lad1-1* cells, no defects in the cell wall or septum were evident prior to the beginning of primary septum dissolution (Fig. 2A). In most wild-type cells, the septum is digested centripetally and new cell tips begin to round as the daughter cells separate (Fig. 2B). However, in *lad1-1* cells septum degradation appeared to initiate at a single position around the cell circumference and the entire cell wall disappeared from this area (Fig. 2C). This lack of cell wall protection at the division site is entirely consistent with the lysis phenotype in which daughter cells pop open at one spot while remaining attached in other areas (see Fig. 1).

Identification of *lad1-1* rescuers

In an attempt to identify the *lad1*$^{+}$ gene, *lad1-1* cells were transformed with a plasmid library and colonies were allowed to form at 25°C. They were then replica-plated to 25°C to remove residual sorbitol and after sizeable colonies had formed, replica-plated a second time to 36°C on rich media. Several colonies grew and plasmids were isolated from them. The recovered plasmids were tested for re-rescue and then checked for sequence relatedness by Southern blotting. Two unrelated gene sequences were identified in these plasmids. Integration mapping, however, revealed that neither gene corresponded to *lad1*$^{+}$ (data not shown). DNA sequencing revealed that one suppressor gene, isolated repeatedly, was *rho1*$^{+}$ (Fig. 3A). The other suppressor gene (Fig.

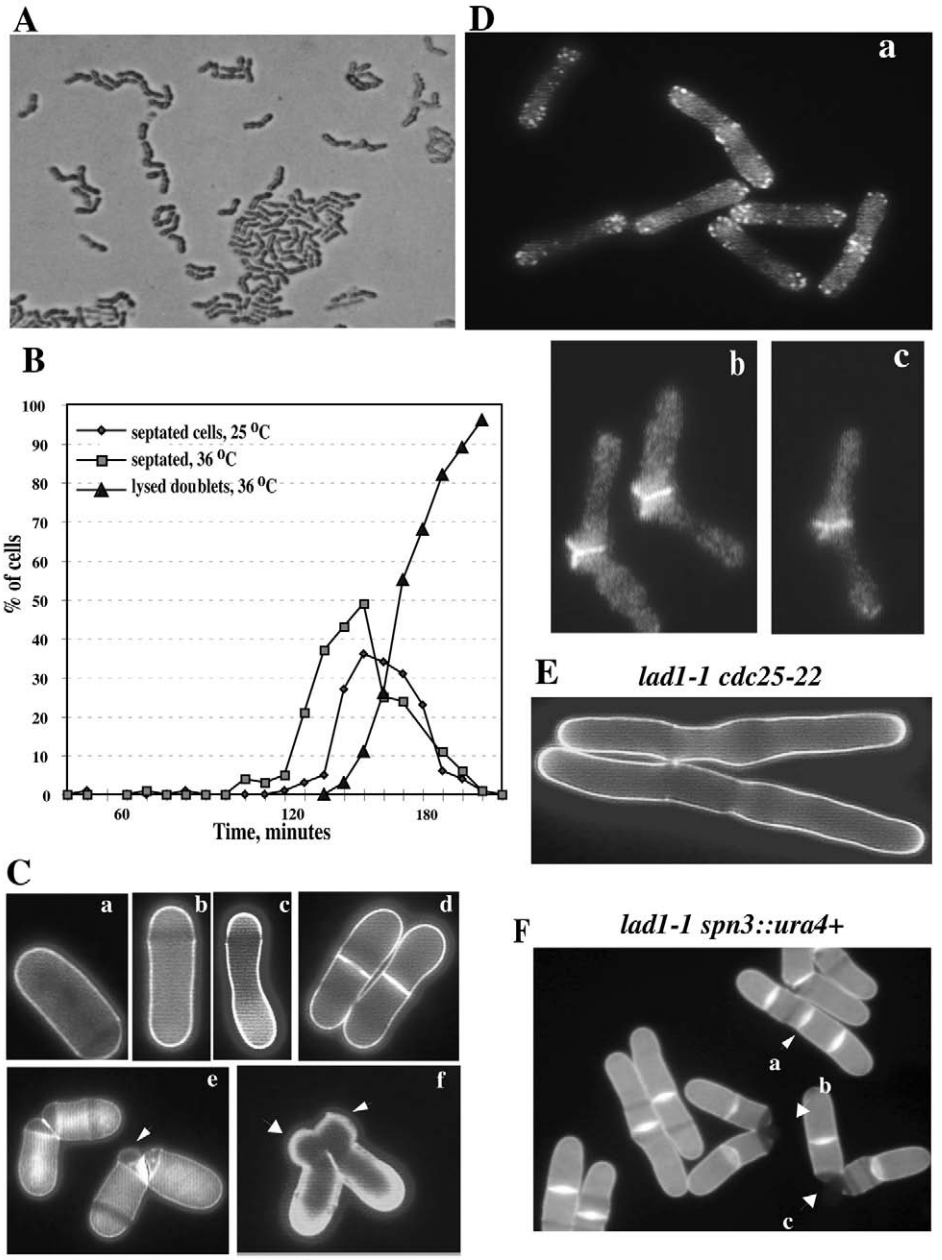

Fig. 1. Phenotype of the *lad1-1* mutant strain. (A) *lad1-1* cells (KGY2030) were grown at 25°C and replica-plated overnight to 36°C. Cells were photographed on the plate. (B-D) *lad1-1* (KGY2030) was grown to mid-exponential phase at 25°C and a synchronous population was isolated by centrifugal elutriation. (B) One portion of the culture was incubated at 25°C and the other at 36°C. The septation index of both cultures was determined microscopically as was the percentage of lysed doublets at the indicated time points. (C) Cells from B incubated at 36°C were stained with calcofluor at 20 (a), 60 (b), 100 (c), 140 (d), 160 (e) and 180 (f) minutes after shifting to 36°C. Arrows indicate extruding or lysing areas of the cells. (D) From the same elutriated culture, samples were collected at 120 (a) or 160 minutes (b and c), fixed with methanol and stained with antibodies to actin (a and b) or Arp3 (c). (E) A double-mutant strain, *cdc25-22 lad1-1* (KGY2041), was grown to mid-exponential phase, shifted to 36°C for 4 hours, and stained with calcofluor. (F) A double mutant strain, *lad1-1 spn3::ura4* (KGY 3944), was shifted to 36°C for 5 hours and stained with calcofluor. Arrows indicate multiseptate cells (a) and multi-septated cells beginning to lyse as cell division proceeds (b and c).

3A), isolated once, corresponded to SPBC651.03c that encodes one of nine putative *S. pombe* Rab GAP that we have named Gyp10p (GAP for Ypt). These proteins are characterized by the presence of a TBC domain (Neuwald, 1997) and an involvement in membrane trafficking events (Pfeffer, 2001). Gyp10p, which is predicted to encode a 43 kDa protein of 373 amino acids, contains a TBC domain at residues 39-242 and a probable transmembrane helix at residues 344-366. Consistent with a role in membrane trafficking, an N-terminal GFP fusion with Gyp10 localized to structures reminiscent of the endoplasmic reticulum (Broughton et al., 1997) when expressed from the low strength *nmt81* promoter (Fig. 3B).

To determine the role of *gyp10*$^+$ in cell division, we examined whether it was an essential gene. Cells deleted for *gyp10*$^+$ (*gyp10Δ*) were able to form colonies at 25-34°C but were severely compromised for growth at 36°C (Fig. 3C). After a shift to 36°C, cells grown in liquid medium accumulated primarily as slightly rounded cells containing two nuclei and a single septum although cells with multiple septa were also detected (Fig. 3D). Consistent with a role in vesicular trafficking, *gyp10Δ* showed a strong negative genetic interaction with cells lacking the exocyst subunit, Exo70p (Wang et al., 2002) (Fig. 3C). At 32°C, the double mutants died with a combination of the *gyp10Δ* and *exo70Δ* phenotypes; they were multi-septated as well as shorter and thicker (data not shown). Overexpression of *gyp10*$^+$ off a plasmid from either its own promoter or the *nmt1* promoter had no discernable phenotype at 25°C (data not shown). However, at 36°C, more *gyp10*$^+$-overexpressing cells contained septa compared with the wild type (15% for pUR18 plasmids vs 10% in the control and 11% for *nmt1* plasmids vs 5% in the control) and ~1-3% accumulated multiple septa (Fig. 3E). This delay in cell separation might account for the ability of *gyp10*$^+$ to rescue *lad1-1* cells at 36°C.

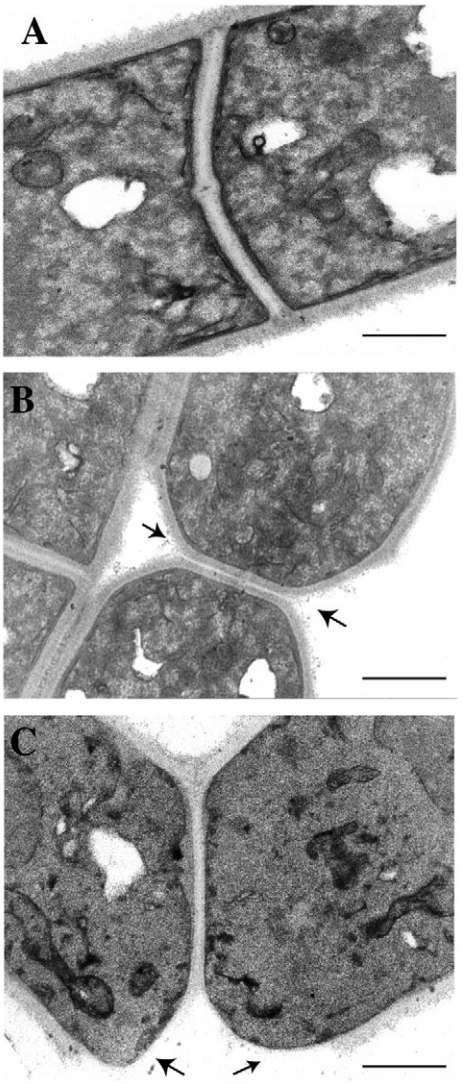

Fig. 2. Electron microscopic analysis of *lad1-1* cells. Electron micrographs of representative wild-type cells (KGY246) (B) and *lad1-1* mutant (KGY2030) cells (A and C) after shifting to 36°C. The arrows in B indicate areas in which the primary septum was degraded. The arrows in C indicate regions lacking cell wall. Bar, 0.9 μm (A,C); 1.0 μm (B).

Mapping of *lad1-1*

Because we were unable to identify the *lad1*$^+$ gene by plasmid complementation, we turned to genetic mapping. Using a long-range mapping strategy that makes use of the meiotic recombination defect of *swi5-39* (Schmidt, 1993), it was determined that *lad1-1* was linked to *ade6*$^+$ on chromosome III. Given its defect in cell separation and its proximity to *ade6*$^+$, *lad1-1* was tested for linkage to *myo2*$^+$ that also resides near *ade6*$^+$ on chromosome III. Out of 15 complete tetrads, not a single recombination event was identified between *lad1-1* and *myo2-E1*; all tetrads were parental ditypes (data not shown). However, the *myo2*$^+$ gene failed to rescue growth of *lad1-1* cells (data not shown) indicating that *lad1-1* was not an allele of *myo2*$^+$. Interestingly, next to *myo2*$^+$ on the chromosome were two adjacent genes, *rgf1*$^+$ and *rgf3*$^+$, predicted to encode Rho-guanine nucleotide exchange factors (Rho-GEFs), the features of which are illustrated in Fig. 4A. Rgf2p is a third highly related Rho-GEF in *S. pombe* (Iwaki et al., 2003). Because *rho1*$^+$ had rescued *lad1-1* cells and the lysis phenotype of *lad1-1* cells resembled that of cells depleted for *rho1*$^+$ (Arellano et al., 1997), it seemed likely to us that the *lad1-1* mutation disrupted the function of *rgf1*$^+$ and/or *rgf3*$^+$.

To help distinguish whether Rgf1p and Rgf3p corresponded to *lad1*$^+$, we decided to examine their intracellular localizations reasoning that the relevant GEF would be found at the division site. For this purpose, the endogenous *rgf1*$^+$ and *rgf3*$^+$ genes were altered to produce C-terminally GFP-tagged variants. Both proteins localized to the division site although their patterns differed (Fig. 4B,D). Rgf1p-GFP formed rings (Fig. 4B) late in mitosis as only cells containing segregated DNA masses contained them (data not shown and Fig. 7A). These rings did not constrict. Rather, Rgf1p-GFP began as a ring (Fig. 4C, upper panels) and then filled in circumferentially with the septum to form a disc (Fig. 4C, lower panels). Rgf1p-GFP was also detected at cell ends (Fig. 4B). By contrast, Rgf3p-GFP was not detected at cell ends, only at the medial region of the cell (Fig. 4D). Furthermore, Rgf3p rings constricted (Fig. 4D, inset). These differences in pattern are illustrated in Fig. 4E.

We next examined whether these localization patterns were disrupted in *lad1-1* cells. For this purpose, the endogenous *rgf1*$^+$ and *rgf3*$^+$ genes were altered to produce C-terminally

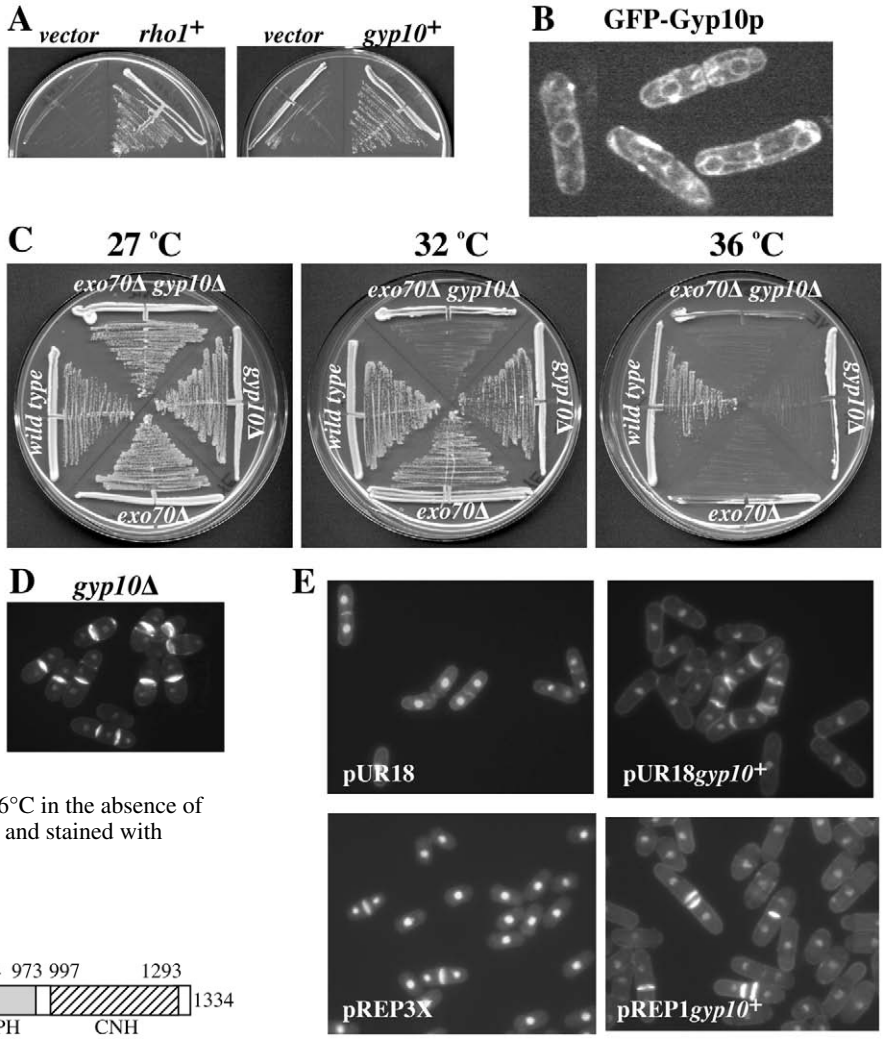

Fig. 3. Identification and characterization of *lad1-1* suppressors. (A) *lad1-1* cells containing pUR19 (vector), pUR19 *rho1* or pUR19*gyp10* were isolated at 25°C and struck to YE plates at 36°C. Colonies were allowed to form for 3 days. (B) The pREP81-GFP*gyp10* plasmid was transformed into wild-type cells (KGY246). After growth of transformants in the absence of thiamine for 16 hours, images of live cells were captured, and a composite of representative cells is shown. (C) Wild-type (KGY246), *gyp10Δ* (KGY2111), *exo70Δ* (MBY919) and *gyp10Δ exo70Δ* (KGY3945) cells were struck to plates for 3 days at the indicated temperatures. (D) *gyp10Δ* cells (KGY2011) were grown at 36°C for 6 hours, fixed, and stained with DAPI and Aniline Blue to visualize DNA and cell wall material, respectively. (E) Wild-type cells (KGY246) were transformed with the indicated plasmids and colonies recovered at 25°C. These were then grown in liquid medium at 36°C in the absence of thiamine for 18 hours. Cells were fixed with ethanol and stained with Aniline Blue and DAPI.

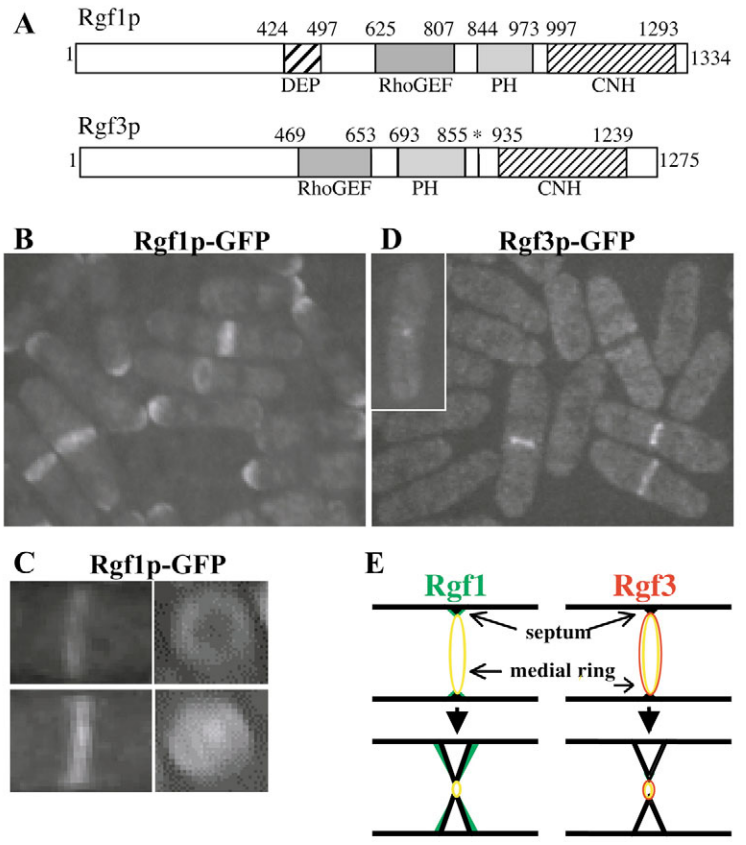

GFP-tagged variants directly in the *lad1-1* strain. At 25°C, both proteins localized normally (Fig. 5A and data not shown). At 36°C, Rgf1p-GFP localization was unaffected by the *lad1-1* mutation (Fig. 5B). By contrast, Rgf3p-GFP failed to localize to any discrete location within the cell (Fig. 5C). This is not due to an inability to detect Rgf3p-GFP at 36°C as it localizes normally at this temperature in wild-type cells (Fig. 5D). Further, we noted that the addition of the GFP tag to Rgf3p exacerbated the lysis phenotype of the cells (data not shown). Consistent with the GFP localization

Fig. 4. Localization of *rgf1*$^+$ and *rgf3*$^+$. (A) Schematic representation of Rgf1 and Rgf3 protein domain structures. Both proteins contain RhoGEF, pleckstrin homology (PH) and citron homology (CNH) domains. In addition, Rgf1 contains a DEP (dishevelled, Egl-10 and pleckstrin) domain. The asterisk denotes the F867S mutation found within *rgf3* in the *lad1-1* strain. (B-D) Localization of Rgf1p-GFP in live cells (B,C) and Rgf3p-GFP in fixed cells (D) (KGY4404 and KGY4407, respectively). (C) The ring of Rgf1p-GFP viewed from the side and en face. (E) Model of Rgf1p and Rgf3p localization during cell division.

data, we found by immunoprecipitation and immunoblotting that Rgf3-GFP from the *lad1-1* strain was reduced in abundance at the permissive temperature and barely detectable after a 2 hour shift to the non-permissive temperature whereas Rgf3-GFP from wild-type cells was easily detected at both temperatures (Fig. 5E, left panel). Moreover, Rgf1-GFP from the *lad1-1* strain was easily detected in these cells when shifted to 36°C (Fig. 5E, right panel). These results were consistent with the possibility that the *lad1-1* mutation generates a mutant Rgf3p. To confirm this hypothesis, overlapping PCR products of the entire *rgf1* and *rgf3* genes from the *lad1-1* strain were generated and sequenced directly. A single mutation was detected in *rgf3* that results in a change of F867 to S867. This mutation is found between the PH and CNH domains (Fig. 4A). No mutations were detected in PCR products generated from *rgf1*. That *lad1-1* represents a novel allele of *rgf3* was further substantiated by the ability of multi-copy *rgf3*$^+$ to rescue the *lad1-1* strain at 36°C (Fig. 5F). Interestingly, overexpression of *gpt10*$^+$ (Fig. 5G), but not *rho1*$^+$ (data not shown) restored the localization of Rgf3 in *lad1-1* cells at 36°C. This suggests that additional Gyp10p might restore the function of mutant Rgf3p by stabilizing it whereas additional Rho1p bypasses the requirement for Rgf3p.

To further distinguish between *rgf1* and *rgf3*, one allele of each gene was replaced with *ura4*$^+$ in independent diploid strains. Tetrad dissection of these strains indicated that *rgf3*$^+$ is essential as only two Ura$^-$ colonies and no Ura$^+$ colonies were obtained in each tetrad (data not shown). By contrast, *rgf1::ura4*$^+$ colonies were recovered indicating that *rgf1*$^+$ is not an essential gene. *rgf1::ura4*$^+$ cells did not display detectable defects in cell division (Fig. 6A). We went on to test for genetic interactions between mutants of *rgf1*, *rgf2*, and *rgf3*. We found that *rgf1::ura4*$^+$ cells were synthetically lethal when combined with the deletion of the highly related *rgf2* gene (Iwaki et al., 2003). In all tetrads analyzed from the cross, tetratypes resulted in three viable colonies and non-parental ditypes gave rise to two viable colonies. No negative genetic interaction was detected between *rgf2:ura4*$^+$ and *lad1-1* (data not shown). Owing to the tight linkage between the *rgf1*$^+$ and *rgf3*$^+$ genes, we did not test for genetic interaction between their mutations.

Given that the lysis phenotype of *lad1-1* is similar to the loss of *rho1*$^+$ (Arellano et al., 1997), we next asked whether Rho1p was able to localize correctly to the medial region of the cell in the *lad1-1* strain that we had shown lacks medially placed Rgf3p (Fig. 5C). We found that it did (Fig. 6B). Thus, the targeting of Rho1p to the medial region can occur in the absence of Rgf3p.

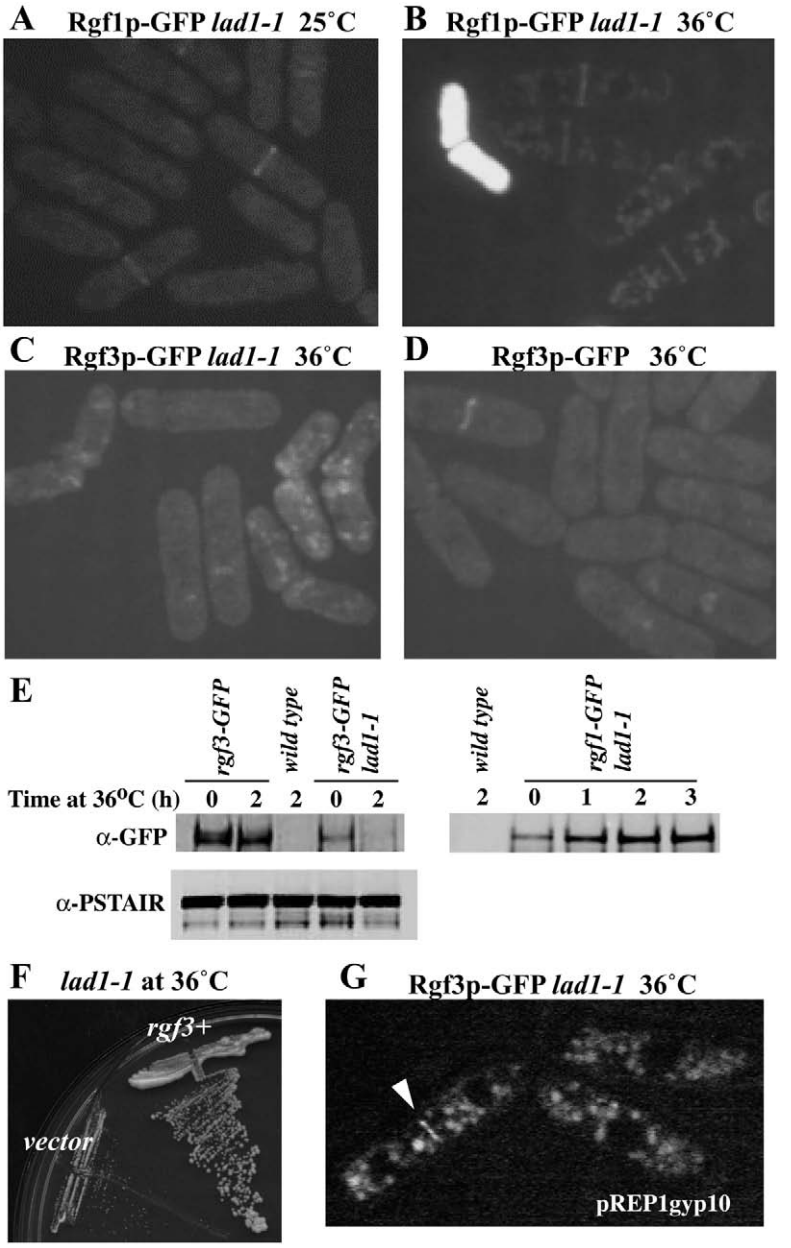

Fig. 5. Localization of Rgf3p but not Rgf1p or Rho1p is disrupted in *lad1-1* cells. (A,B) *rgf1-GFP lad1-1* cells (KGY1116) were grown at 25°C (A) and then shifted to 36°C for 4 hours (B). (C,D) *rgf3-GFP lad1-1* (KGY1117) (C) and *rgf3-GFP* cells (KGY4407) (D) cells were grown at 25°C and then shifted to 36°C for 4 hours. Images of live cells are shown in each panel. (D) The same strains grown in parts A-D were grown at 25°C and shifted to 36°C for 0 or 2 hours and equal amounts of cell lysates were probed for Cdc2p levels using anti-PSTAIRE, or immunoprecipitated and immunoblotted with antibodies to GFP. (F) *lad1-1* cells containing pREP1 (vector) or pREP1*rgf3*$^+$ were isolated at 25°C and struck to YE plates at 36°C. Colonies were allowed to form for 3 days. (G) *rgf3-GFP lad1-1* cells (KGY1117) were transformed with pREP1gyp10 and colonies were allowed to form at 25°C. Transformants were grown in liquid medium lacking thiamine for 18 hours and then shifted to 36°C for 3 hours. Live cell images were captured. The arrowhead indicates the Rgf3-GFP medial ring.

The lysis phenotype of *lad1-1* cells is very reminiscent of hypomorphic mutations in components of the SIN. Therefore, we examined double mutants of *lad1-1* with a large variety of mutations in SIN genes. No additive effects were detected (data not shown). We also examined whether either Rgf3p or Rgf1p

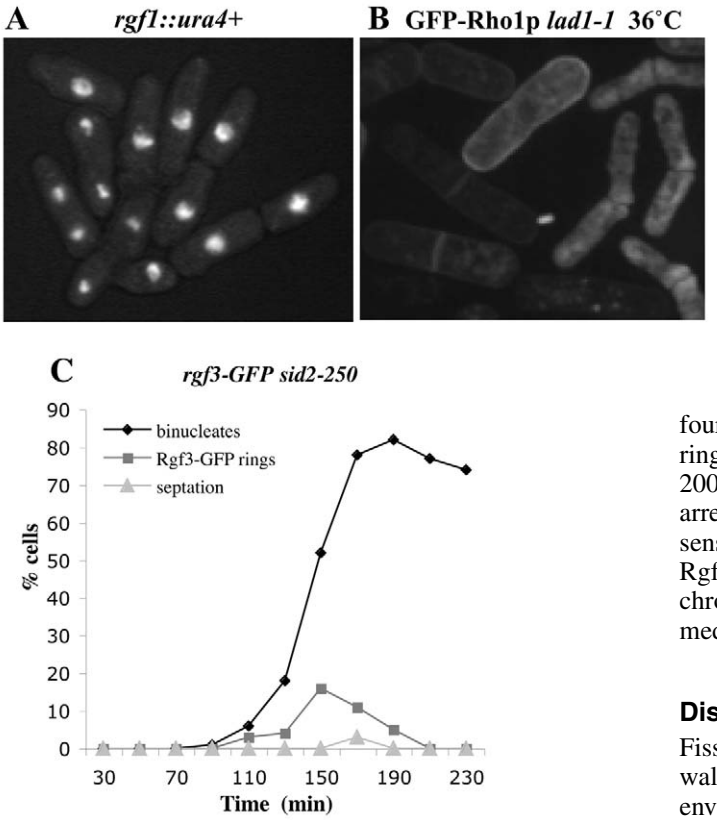

Fig. 6. Rgf3 is independent of the SIN. (A) The *rgf1::ura4*$^{+}$ strain (KGY 5385) was grown at 32°C in YE, fixed with ethanol, and stained with DAPI. (B) pARTGFP-Rho1 was transformed into *lad1-1* cells. Transformants were grown at 25°C, filtered and resuspended in YE medium and shifted to 36°C for 4 hours. GFP-Rho1p localization was visualized in live cells. Arrowheads indicate medially localized GFP-Rho1p. (C) *rgf3-GFP sid2-250* cells (KGY5326) were synchronized in G2 phase by lactose gradient centrifugation, filtered, resuspended in fresh medium at 36°C and followed throughout a cell cycle. The percentage of binucleate (anaphase) cells, septated cells and cells with Rgf3p-GFP rings were determined every 20 minutes.

depended upon SIN function for medial ring localization and found that neither did (Fig. 6C and data not shown). Reciprocally, the Sid2p kinase was found to localize normally in *lad1-1* cells (data not shown). Therefore, the lysis phenotypes of SIN and *rgf3* mutations, although appearing similar, are probably due to distinct perturbations of the cell division process, one occurring early (SIN) and the other late (*lad1-1*).

Through the cell cycle *rgf3*$^{+}$ mRNA oscillates in abundance (Tajadura et al., 2004) and microarray analyses indicate that *rgf3*$^{+}$ is upregulated at late mitosis (Peng et al., 2005; Rustici et al., 2004). Like *rgf3*$^{+}$ mRNA (Tajadura et al., 2004), we found that Rgf3p began to accumulate as cells entered mitosis and peaked in abundance during septation (Fig. 7A). Cluster analysis of microarray data indicated that *rgf3*$^{+}$ transcription is controlled by the transcription factor, Ace2p (Peng et al., 2005; Rustici et al., 2004), that plays a key role in orchestrating cell separation in both fission and budding yeasts (Martin-Cuadrado et al., 2003; O'Conallain et al., 1999). In fission yeast, at least seven true Ace2p targets have been studied and all accumulate at the onset of anaphase (Alonso-Nunez et al., 2005; Tasto et al., 2003). To determine whether Rgf3p production was controlled by Ace2p, we examined whether Rgf3p levels were altered in cells lacking or overproducing Ace2p. Overproduction of Ace2p led to increased Rgf3p levels whereas Rgf3p was less abundant in cells lacking Ace2p (Fig. 7B). However, Rgf3p-Myc$_{13}$ was clearly detectable in the absence of Ace2p suggesting that other factors cooperate with Ace2p to regulate *rgf3*$^{+}$ expression. Consistent with this, we found that Rgf3p-GFP began to appear at the medial region of cells prior to anaphase (Fig. 7C). This behavior contrasts with four Ace2p targets previously analyzed that accumulate at the ring only in anaphase (Alonso-Nunez et al., 2005; Tasto et al., 2003). Indeed, Rgf3p-GFP could be detected readily in cells arrested in a metaphase-like state with the *nda3-km311* cold-sensitive tubulin mutant (Fig. 7D,E). In contrast to Rgf3p, Rgf1p was detected at the medial region of cells only after chromosome segregation (Fig. 7F) and was not observed at the medial region of arrested *nda3-km311* cells (data not shown).

Discussion

Fission yeast, like other yeast, are surrounded by a rigid cell wall that provides mechanical strength and protection from environmental stresses (Cabib et al., 1997). The wall is required for the formation and maintenance of cell shape and is remodeled continuously during the cell cycle to allow cell expansion and division. Cell wall remodeling also occurs in response to extracellular cues that trigger shape changes, such as nutrient deprivation and exposure to mating factors. Our data indicate that the Rho-GEF, Rgf3p, is essential for the cell wall remodeling that accompanies cell division, specifically to protect the new cell ends created by digestion of the primary septum.

The *S. pombe* cell wall is comprised largely of the carbohydrates α-galactomannans, α-(1,3)-, β-(1,6)- and β(1,3)-linked glucans with β-(1,3)-linked glucans comprising the majority of cell wall polysaccharide (reviewed by Perez and Ribas, 2004). The Rho1 GTPase is an essential activator of glucan synthase activity in both *S. pombe* and *S. cerevisiae* (reviewed by Arellano et al., 1999) and therefore it is not surprising that loss of a Rho1p activator would lead to defects in cell wall integrity. Indeed, loss of Rho1p in *S. pombe* leads to similar defects in cell division as the loss of Rgf3p activity. Our isolation of *rho1*$^{+}$ repeatedly as a multi-copy suppressor of *lad1-1* cell lysis but not any of the other *S. pombe rho* genes provides genetic evidence that Rgf3p activates Rho1p specifically. Biochemical evidence for the selective action of Rgf3p on Rho1p was reported by Tajadura and colleagues while this manuscript was in preparation (Tajadura et al., 2004). Indeed, these authors isolated another mutation within *rgf3* in a screen for hypersensitivity to drugs that inhibit cell wall biosynthesis (Tajadura et al., 2004). The phenotype of this mutation within *rgf3* (*ehs2-1*) is indistinguishable from *lad1-1* although the alleles contain different mutations.

Not explained from our analyses or that of Tajadura and colleagues is the selective defect in cell wall integrity at division in cells lacking Rgf3p. We have shown by light and

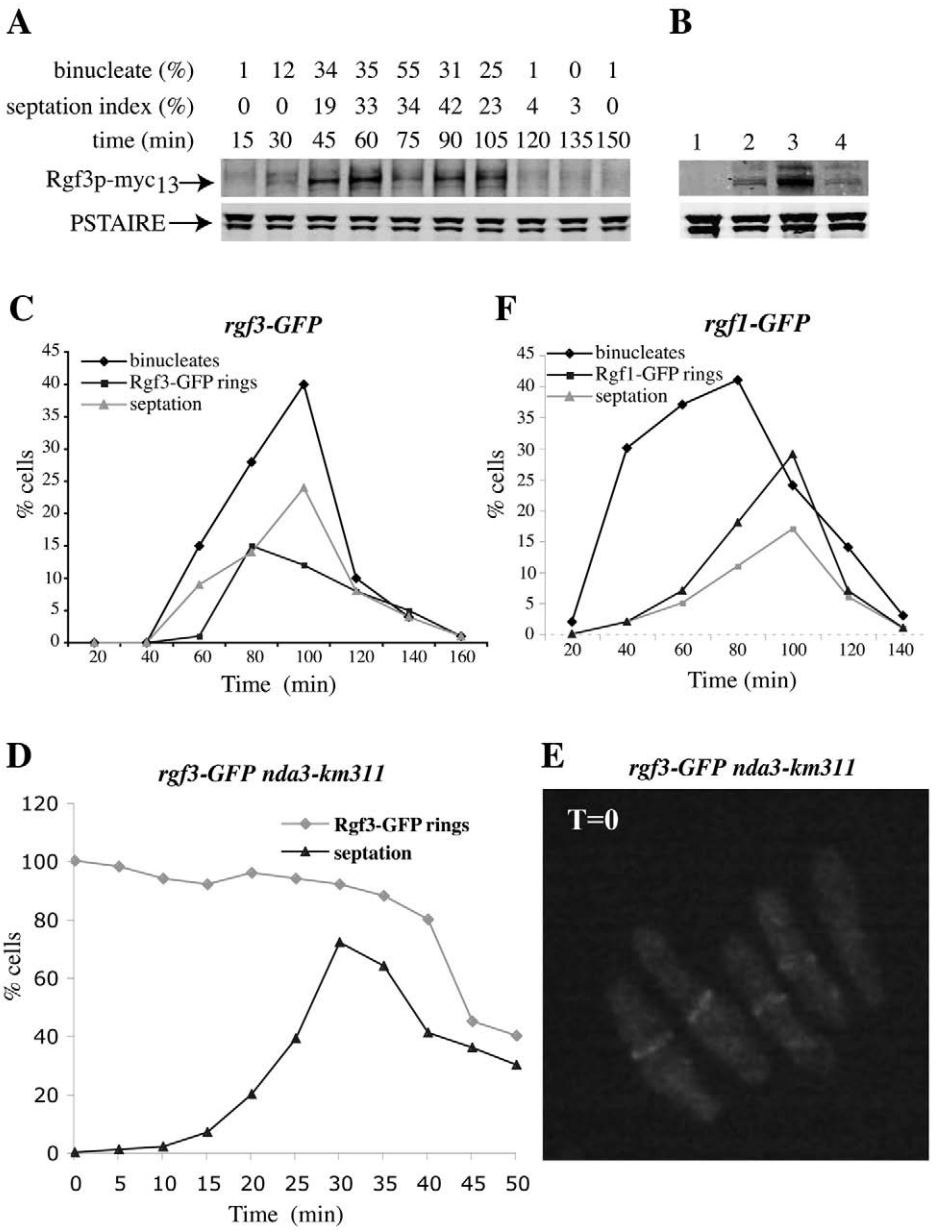

Fig. 7. Rgf3p localizes early in mitosis. (A) Rgf3p-Myc$_{13}$ cells (KGY4401) were grown to mid-log phase at 32°C in YE medium, and synchronized in early G2 phase by centrifugal elutriation. Samples were collected every 15 minutes and analyzed for the abundance of Rgf3p-Myc$_{13}$ by immunoblotting of denatured cell protein lysates. Blotting with anti-PSTAIRE to Cdc2p from the same immunoblot served as a loading control. The septation index and the percentage of binucleate (anaphase) cells were also measured at each time point. (B) The level of Rgf3p-Myc$_{13}$ was determined in log-phase wild type cells (KGY246) (lane 1), *rgf3-myc$_{13}$* (KGY4401) (lane 2), *rgf3-myc$_{13}$ ace2::kan^{R}* (KGY5160) (lane 3) and *rgf3-myc$_{13}$* overproducing Ace2p from the *nmt1* promoter (lane 4) was determined by immunoblotting of denatured protein lysates. The abundance of Cdc2p determined by immunoblotting the same protein gel with anti-PSTAIRE served as a loading control. (C) *rgf3-GFP* cells (KGY4407) synchronized in G2 phase by lactose gradient centrifugation and followed throughout a cell cycle. The percentage of binucleate (anaphase) cells, septated cells, and cells with Rgf3p-GFP rings were determined every 20 minutes. (D and E) *rgf3-GFP nda3-km311* cells (KGY5400) were arrested by incubation at 19°C for 6 hours and released at time 0 by shift to 32°C. Samples were fixed in ethanol every 5 minutes to determine the percentage of cells with Rgf3p-GFP rings and a septum (D). (E) A representative image of these cells at the arrest point. (F) *rgf1-GFP* cells (KGY4407) were synchronized in G2 phase by lactose gradient centrifugation and followed throughout a cell cycle. The percentage of binucleate (anaphase) cells, septated cells and cells with Rgf1p-GFP rings were determined every 20 minutes.

electron microscopy that these cells display normal morphology and growth during interphase, and that they form primary and secondary septa normally. Further, in a septin mutant that is delayed in cell separation, *lad1-1* cells can undergo another cell cycle to form three septa without lysis. It is only when primary septum degradation begins that Rgf3p plays an essential function in maintaining cell wall integrity. Three glucan synthases are responsible for cell wall deposition during vegetative growth, Cps1p (Ishiguro et al., 1997; Le Goff et al., 1999b; Liu et al., 1999), Bgs3p (Martin et al., 2003) and Bgs4p (Cortes et al., 2005). It was reported that total glucan synthase activity is reduced by half in the absence of *rgf3*$^{+}$ (Tajadura et al., 2004). Given Rgf3p cell cycle periodicity, its restricted localization at the medial region and the lack of overall morphology changes in *rgf3*$^{+}$ mutants, this is a larger-than-expected effect. However, it seems clear that Rgf3p is critically rate limiting for Rho1p-mediated stimulation of glucan synthase activity during cell separation. It is noteworthy in this regard that Bgs4p activity is particularly crucial at this stage in the cell cycle as well; cells lacking *bgs4*$^{+}$ lyse frequently at the junction between septum and old cell wall (Cortes et al., 2005), a phenotype similar to the loss of Rho1p and the loss of Rgf3p. Thus, Rgf3p might be essential for Rho1p-stimulated Bgs4p activation during cytokinesis and two other highly related Rho-GEFs, Rgf1p and Rgf2p (Iwaki et al., 2003) might provide redundant Rho1p-mediated glucan synthase activation throughout the remainder of the cell cycle. That overproduction of Rgf3p leads to a delay in cell separation and the formation of multi-nucleate and multi-septated cells but does not phenocopy Rho1p overproduction (Iwaki et al., 2003; Tajadura et al., 2004) is consistent with this possibility.

Rgf3p is one of seven Rho-GEFs encoded by the *S. pombe* genome (Iwaki et al., 2003). Whereas Scd1p and Gef1p are specific for Cdc42p (Chang et al., 1994; Coll et al., 2003;

Hirota et al., 2003), Rgf3p is specific for Rho1p (Tajadura et al., 2004) and is more closely related to Rgf1p and Rgf2p than the other Rho-GEF proteins (Iwaki et al., 2003). Given that there are four other Rho proteins (Rho2-Rho5) (Hirata et al., 1998; Nakano et al., 2002; Nakano et al., 2003; Santos et al., 2003; Wang et al., 2003) and several biochemically uncharacterized GEFs (Iwaki et al., 2003), it will take considerable effort in the future to sort out the biochemical specificities, cellular roles, and regulation of each Rho-GEF. In an effort to begin characterizing these proteins, Iwaki and colleagues deleted and overproduced the genes encoding all of them in fission yeast cells (Iwaki et al., 2003). Consistent with their results, we found that *rgf1*$^+$ was not an essential gene and *rgf1::ura4*$^+$ cells were morphologically similar to the wild type. However, we found that the deletion of both *rgf1*$^+$ and *rgf2*$^+$ was synthetically lethal suggesting that they participate in a common essential function. Rgf1p localizes to cell ends during interphase and the division site late in anaphase, a very different pattern from Rgf3p, suggesting non-overlapping functions. Consistent with this, our results indicate, as do those of Tajadura and colleagues (Tajadura et al., 2004), that *rgf3*$^+$ is an essential gene. Given the tight linkage between *rgf1*$^+$ and *rgf3*$^+$, it is not possible to create a double mutant strain (*lad1-1 rgf1::ura4*$^+$) in order to easily investigate possible redundancy in function of Rgf3p and Rgf1p. However, a double mutant (*lad1-1 rgf2::ura4*$^+$) did not show a reduction in restrictive temperature, a result also consistent with the idea that Rgf3p function is distinct from that of Rgf1p and Rgf2p.

Microarray analyses (Peng et al., 2005; Rustici et al., 2004) and conventional northern analysis (Tajadura et al., 2004) reveal that *rgf3*$^+$ RNA oscillates in abundance through the cell cycle. Cluster analysis suggested that the Ace2p transcription factor participates in its expression (Peng et al., 2005; Rustici et al., 2004) although microarray analysis aimed at detecting Ace2p regulated genes did not identify *rgf3*$^+$ as a major target (Alonso-Nunez et al., 2005). We found that Rgf3p levels were significantly reduced in cells lacking Ace2p and increased in cells overproducing Ace2p. Taken together these results suggest that Ace2p plays an important role in regulating the levels of this Rho-GEF indicating another manner in which Ace2p controls the latter stages of cell separation in *S. pombe*.

The *rgf3* mutation in *lad1-1* that falls between the PH and CNH domains, not within the GEF domain, prevents Rgf3p from localizing to the medial ring during cytokinesis, and causes significant instability of the protein. Our isolation of *gyp10*$^+$ as a high-copy suppressor of *lad1-1* might be meaningful in this regard. Gyp10 is a previously uncharacterized Rab GAP that is presumably involved in vesicular trafficking, a hypothesis supported by the negative genetic interaction observed between the *gyp10* and *exo70* mutations. Gyp10p overproduction appears to stabilize Rgf3p and drives its recruitment to membranes. This might occur by increasing the local concentration of an interacting protein.

Although the essential function of Rgf3p has been pinpointed to the beginning of cell separation, it is interesting that it is present in the cytokinetic ring prior to anaphase (Fig. 6) and that Rho1p also joins the ring prior to septation (Nakano et al., 1997). The role of Rho proteins in cytokinesis has been clearly established in other organisms that do not require cell wall synthesis (reviewed by Prokopenko et al., 2000). Moreover, the Rho-GEF Pbl/ECT2 is essential for cytokinetic furrow formation in several organisms (reviewed by Glotzer, 2004). That they are present in the ring prior to septation would be consistent with Rgf3p-Rho1p participating in events of cell division independent of maintaining cell wall integrity. Further study of Rgf3p-interacting proteins might be revealing as to their other possible roles in cytokinesis.

We would like to acknowledge Mohan Balasubramanian for suggesting the isolation of mutants based on NaF sensitivity performed years ago and Seung-Joo Lee for technical assistance. We are grateful to Issei Mabuchi for providing the pARTGFPRho1 plasmid, Masaaki Miyamoto for providing the pREP1*rgf3*$^+$ plasmid, Claudia Petit and Srinivas Venkatram for helpful comments on the manuscript, and Mohan Balasubramanian and Masaaki Miyamoto for providing strains used in this study. This work was supported by the HHMI of which K.L.G. is an investigator.

References

Alonso-Nunez, M. L., An, H., Martin-Cuadrado, A. B., Mehta, S., Petit, C., Sipiczki, M., Del Rey, F., Gould, K. L. and Vazquez de Aldana, C. R. (2005). Ace2p controls the expression of genes required for cell separation in *Schizosaccharomyces pombe*. *Mol. Biol. Cell* **16**, 2003-2017.

An, H., Morrell, J. L., Jennings, J. L., Link, A. J. and Gould, K. L. (2004). Requirements of fission yeast septins for complex formation, localization, and function. *Mol. Biol. Cell* **15**, 5551-5564.

Arellano, M., Duran, A. and Perez, P. (1997). Localisation of the *Schizosaccharomyces pombe* rho1p GTPase and its involvement in the organisation of the actin cytoskeleton. *J. Cell Sci.* **110**, 2547-2555.

Arellano, M., Coll, P. M. and Perez, P. (1999). RHO GTPases in the control of cell morphology, cell polarity, and actin localization in fission yeast. *Microsc. Res. Tech.* **47**, 51-60.

Bahler, J., Wu, J. Q., Longtine, M. S., Shah, N. G., McKenzie, A., 3rd, Steever, A. B., Wach, A., Philippsen, P. and Pringle, J. R. (1998). Heterologous modules for efficient and versatile PCR-based gene targeting in *Schizosaccharomyces pombe*. *Yeast* **14**, 943-951.

Balasubramanian, M. K., McCollum, D. and Gould, K. L. (1997). Cytokinesis in fission yeast *Schizosaccharomyces pombe*. *Methods Enzymol.* **283**, 494-506.

Balasubramanian, M. K., Bi, E. and Glotzer, M. (2004). Comparative analysis of cytokinesis in budding yeast, fission yeast and animal cells. *Curr. Biol.* **14**, R806-R818.

Barbet, N. C. and Carr, A. M. (1993). Fission yeast wee1 protein kinase is not required for DNA damage- dependent mitotic arrest. *Nature* **364**, 824-827.

Barbet, N., Muriel, W. J. and Carr, A. M. (1992). Versatile shuttle vectors and genomic libraries for use with *Schizosaccharomyces pombe*. *Gene* **114**, 59-66.

Berlin, A., Paoletti, A. and Chang, F. (2003). Mid2p stabilizes septin rings during cytokinesis in fission yeast. *J. Cell Biol.* **160**, 1083-1092.

Broughton, J., Swennen, D., Wilkinson, B. M., Joyet, P., Gaillardin, C. and Stirling, C. J. (1997). Cloning of SEC61 homologues from Schizosaccharomyces pombe and Yarrowia lipolytica reveals the extent of functional conservation within this core component of the ER translocation machinery. *J. Cell Sci.* **110**, 2715-2727.

Cabib, E., Drgon, T., Drgonova, J., Ford, R. A. and Kollar, R. (1997). The yeast cell wall, a dynamic structure engaged in growth and morphogenesis. *Biochem. Soc. Trans.* **25**, 200-204.

Chang, E. C., Barr, M., Wang, Y., Jung, V., Xu, H. P. and Wigler, M. H. (1994). Cooperative interaction of *S. pombe* proteins required for mating and morphogenesis. *Cell* **79**, 131-141.

Coll, P. M., Trillo, Y., Ametzazurra, A. and Perez, P. (2003). Gef1p, a new guanine nucleotide exchange factor for Cdc42p, regulates polarity in *Schizosaccharomyces pombe*. *Mol. Biol. Cell* **14**, 313-323.

Cortes, J. C., Carnero, E., Ishiguro, J., Sanchez, Y., Duran, A. and Ribas, J. C. (2005). The novel fission yeast (1,3)beta-D-glucan synthase catalytic subunit Bgs4p is essential during both cytokinesis and polarized growth. *J. Cell Sci.* **118**, 157-174.

Dekker, N., Speijer, D., Grun, C. H., van den Berg, M., de Haan, A. and Hochstenbach, F. (2004). Role of the alpha-glucanase Agn1p in fission-yeast cell separation. *Mol. Biol. Cell* **15**, 3903-3914.

Glotzer, M. (2004). Cleavage furrow positioning. *J. Cell Biol.* **164**, 347-351.
Gould, K. L., Moreno, S., Owen, D. J., Sazer, S. and Nurse, P. (1991). Phosphorylation at Thr167 is required for *Schizosaccharomyces pombe* p34cdc2 function. *EMBO J.* **10**, 3297-3309.
Hall, P. A. and Russell, S. E. (2004). The pathobiology of the septin gene family. *J. Pathol.* **204**, 489-505.
Hirata, D., Nakano, K., Fukui, M., Takenaka, H., Miyakawa, T. and Mabuchi, I. (1998). Genes that cause aberrant cell morphology by overexpression in fission yeast: a role of a small GTP-binding protein Rho2 in cell morphogenesis. *J. Cell Sci.* **111,** 149-159.
Hirota, K., Tanaka, K., Ohta, K. and Yamamoto, M. (2003). Gef1p and Scd1p, the Two GDP-GTP exchange factors for Cdc42p, form a ring structure that shrinks during cytokinesis in Schizosaccharomyces pombe. *Mol. Biol. Cell* **14**, 3617-3627.
Humbel, B. M., Konomi, M., Takagi, T., Kamasawa, N., Ishijima, S. A. and Osumi, M. (2001). In situ localization of β-glucans in the cell wall of *Schizosaccharomyces pombe*. *Yeast* **18**, 433-444.
Ishiguro, J., Saitou, A., Duran, A. and Ribas, J. C. (1997). *cps1+*, a *Schizosaccharomyces pombe* gene homolog of *Saccharomyces cerevisiae* FKS genes whose mutation confers hypersensitivity to cyclosporin A and papulacandin B. *J. Bacteriol.* **179**, 7653-7662.
Iwaki, N., Karatsu, K. and Miyamoto, M. (2003). Role of guanine nucleotide exchange factors for Rho family GTPases in the regulation of cell morphology and actin cytoskeleton in fission yeast. *Biochem. Biophys. Res. Commun.* **312**, 414-420.
Keeney, J. B. and Boeke, J. D. (1994). Efficient targeted integration at leu1-32 and ura4-294 in *Schizosaccharomyces pombe*. *Genetics* **136**, 849-856.
Krapp, A., Gulli, M. P. and Simanis, V. (2004). SIN and the art of splitting the fission yeast cell. *Curr. Biol.* **14**, R722-R730.
Le Goff, X., Utzig, S. and Simanis, V. (1999a). Controlling septation in fission yeast: finding the middle, and timing it right. *Curr. Genet.* **35**, 571-584.
Le Goff, X., Woollard, A. and Simanis, V. (1999b). Analysis of the *cps1* gene provides evidence for a septation checkpoint in *Schizosaccharomyces pombe*. *Mol. Gen. Genet.* **262**, 163-172.
Liu, J., Wang, H., McCollum, D. and Balasubramanian, M. K. (1999). Drc1p/Cps1p, a 1,3-beta-glucan synthase subunit, is essential for division septum assembly in *Schizosaccharomyces pombe*. *Genetics* **153**, 1193-1203.
Martin, V., Garcia, B., Carnero, E., Duran, A. and Sanchez, Y. (2003). Bgs3p, a putative 1,3-beta-glucan synthase subunit, is required for cell wall assembly in *Schizosaccharomyces pombe*. *Eukaryot. Cell* **2**, 159-169.
Martin-Cuadrado, A. B., Duenas, E., Sipiczki, M., De Aldana, C. R. and Del Rey, F. (2003). The endo-beta-1,3-glucanase eng1p is required for dissolution of the primary septum during cell separation in *Schizosaccharomyces pombe*. *J. Cell Sci.* **116**, 1689-1698.
Maundrell, K. (1993). Thiamine-repressible expression vectors pREP and pRIP for fission yeast. *Gene* **123**, 127-130.
McCollum, D. and Gould, K. L. (2001). Timing is everything: regulation of mitotic exit and cytokinesis by the MEN and SIN. *Trends Cell Biol.* **11**, 89-95.
McCollum, D., Feoktistova, A., Morphew, M., Balasubramanian, M. and Gould, K. L. (1996). The *Schizosaccharomyces pombe* actin-related protein, Arp3, is a component of the cortical actin cytoskeleton and interacts with profilin. *EMBO J.* **15**, 6438-6446.
Moreno, S., Klar, A. and Nurse, P. (1991). Molecular genetic analysis of fission yeast *Schizosaccharomyces pombe*. *Methods Enzymol.* **194**, 795-823.
Nakano, K., Arai, R. and Mabuchi, I. (1997). The small GTP-binding protein Rho1 is a multifunctional protein that regulates actin localization, cell polarity, and septum formation in the fission yeast *Schizosaccharomyces pombe*. *Genes Cells* **2**, 679-694.
Nakano, K., Imai, J., Arai, R., Toh, E. A., Matsui, Y. and Mabuchi, I. (2002). The small GTPase Rho3 and the diaphanous/formin For3 function in polarized cell growth in fission yeast. *J. Cell Sci.* **115**, 4629-4639.
Nakano, K., Mutoh, T., Arai, R. and Mabuchi, I. (2003). The small GTPase Rho4 is involved in controlling cell morphology and septation in fission yeast. *Genes Cells* **8**, 357-370.
Neuwald, A. F. (1997). A shared domain between a spindle assembly checkpoint protein and Ypt/Rab-specific GTPase-activators. *Trends Biochem. Sci.* **22**, 243-244.
O'Conallain, C., Doolin, M. T., Taggart, C., Thornton, F. and Butler, G. (1999). Regulated nuclear localisation of the yeast transcription factor Ace2p controls expression of chitinase (CTS1) in Saccharomyces cerevisiae. *Mol. Gen. Genet.* **262**, 275-282.
Peng, X., Karuturi, R. K., Miller, L. D., Lin, K., Jia, Y., Kondu, P., Wang, L., Wong, L. S., Liu, E. T., Balasubramanian, M. K. et al. (2005). Identification of cell cycle-regulated genes in fission yeast. *Mol. Biol. Cell* **16**, 1026-1042.
Perez, P. and Ribas, J. C. (2004). Cell wall analysis. *Methods* **33**, 245-251.
Pfeffer, S. R. (2001). Rab GTPases: specifying and deciphering organelle identity and function. *Trends Cell. Biol.* **11**, 487-491.
Prentice, H. L. (1992). High efficiency transformation of *Schizosaccharomyces pombe* by electroporation. *Nucleic Acids Res.* **20**, 621.
Prokopenko, S. N., Saint, R. and Bellen, H. J. (2000). Untying the Gordian knot of cytokinesis. Role of small G proteins and their regulators. *J. Cell Biol.* **148**, 843-848.
Rustici, G., Mata, J., Kivinen, K., Lio, P., Penkett, C. J., Burns, G., Hayles, J., Brazma, A., Nurse, P. and Bahler, J. (2004). Periodic gene expression program of the fission yeast cell cycle. *Nat. Genet.* **36**, 809-817.
Santos, B., Gutierrez, J., Calonge, T. M. and Perez, P. (2003). Novel Rho GTPase involved in cytokinesis and cell wall integrity in the fission yeast *Schizosaccharomyces pombe*. *Eukaryot. Cell* **2**, 521-533.
Schmidt, H. (1993). Effective long range mapping in *Schizosaccharomyces pombe* with the help of swi5. *Curr. Genet.* **24**, 271-273.
Sipiczki, M., Grallert, B. and Miklos, I. (1993). Mycelial and syncytial growth in *Schizosaccharomyces pombe* induced by novel septation mutations. *J. Cell Sci.* **104**, 485-493.
Sugiura, R., Toda, T., Shuntoh, H., Yanagida, M. and Kuno, T. (1998). pmp1+, a suppressor of calcineurin deficiency, encodes a novel MAP kinase phosphatase in fission yeast. *EMBO J.* **17**, 140-148.
Tajadura, V., Garcia, B., Garcia, I., Garcia, P. and Sanchez, Y. (2004). *Schizosaccharomyces pombe* Rgf3p is a specific Rho1 GEF that regulates cell wall beta-glucan biosynthesis through the GTPase Rho1p. *J. Cell Sci.* **117**, 6163-6174.
Tasto, J. J., Morrell, J. L. and Gould, K. L. (2003). An anillin homologue, Mid2p, acts during fission yeast cytokinesis to organize the septin ring and promote cell separation. *J. Cell Biol.* **160**, 1093-1103.
Toda, T., Dhut, S., Superti-Furga, G., Gotoh, Y., Nishida, E., Sugiura, R. and Kuno, T. (1996). The fission yeast *pmk1+* gene encodes a novel mitogen-activated protein kinase homolog which regulates cell integrity and functions coordinately with the protein kinase C pathway. *Mol. Cell. Biol.* **16**, 6752-6764.
Wang, H., Tang, X., Liu, J., Trautmann, S., Balasundaram, D., McCollum, D. and Balasubramanian, M. K. (2002). The multiprotein exocyst complex is essential for cell separation in *Schizosaccharomyces pombe*. *Mol. Biol. Cell* **13**, 515-529.
Wang, H., Tang, X. and Balasubramanian, M. K. (2003). Rho3p regulates cell separation by modulating exocyst function in Schizosaccharomyces pombe. *Genetics* **164**, 1323-1331.
Wolfe, B. A. and Gould, K. L. (2005). Split decisions: coordinating cytokinesis in yeast. *Trends Cell. Biol.* **15**, 10-18.
Yoshida, T., Toda, T. and Yanagida, M. (1994). A calcineurin-like gene ppb1+ in fission yeast: mutant defects in cytokinesis, cell polarity, mating and spindle pole body positioning. *J. Cell Sci.* **107**, 1725-1735.